INTERNATIONAL JOURNAL FOR NUMERICAL METHODS IN FLUIDS
Int. J. Numer. Meth. Fluids 2008; **56**:1375–1381
Published online 7 August 2007 in Wiley InterScience (www.interscience.wiley.com). DOI: 10.1002/fld.1573

The efficient and accurate solution of continuous thin film flow over surface patterning and past occlusions

Y. C. Lee, H. M. Thompson and P. H. Gaskell*, †

School of Mechanical Engineering, University of Leeds, West Yorkshire LS2 9JT, U.K.

SUMMARY

The benefits of a spatially and time-adaptive full approximation storage (FAS) multigrid method for the solution of the thin film lubrication equations, as used to model gravity-driven flow over complex submerged topography and past small-scale occlusions, are investigated. Results are presented which demonstrate how flow orientation has a significant effect on the magnitude of the resultant free-surface disturbances and how reduction of the in-plane dimensions of the associated topography increases the computational resources needed to achieve grid-independent solutions. In addition, the ability to automatically restrict fine grid resolution only to those regions in and around small, localized topography is shown to lead to significantly increased computational efficiency over grid-independent solutions obtained on globally fine meshes with the same degree of accuracy. Copyright © 2007 John Wiley & Sons, Ltd.

Received 2 April 2007; Revised 18 June 2007; Accepted 18 June 2007

KEY WORDS: finite difference methods; differential equations; adaptivity; mesh adaptation; free surface; micro-fluids; thin film flow; multigrid; surface patterning

1. INTRODUCTION

The flow of continuous thin liquid films over substrates containing regions of micro- or nano-scale heterogeneity is of enormous significance in many natural, engineering and manufacturing systems [1, 2]. They present extremely challenging practical design problems to experimentalists and theoreticians alike since the free-surface disturbances caused by small-scale surface patterning or occlusions can persist over length scales several orders of magnitude greater than their actual size [2]. Historically, the study of such three-dimensional flows has been confined to cases with simple topographic features whose in-plane length scales are of the order of millimetres—significantly larger than those encountered in practice on, for example, leaf surfaces [1] or in the production of micro-scale electronic components [3].

*Correspondence to: P. H. Gaskell, School of Mechanical Engineering, University of Leeds, West Yorkshire LS2 9JT, U.K.
†E-mail: p.h.gaskell@leeds.ac.uk

The focus here is on the efficient numerical solution of such free-surface flows, an area which, despite recent progress, is still in its infancy. Previous analyses have been aided by the fact that in most cases the Reynolds number is small, so the numerical challenge reduces to one of solving Stokes equations. In such cases, the boundary element method has been proven to be effective [4, 5]. However, by far the most popular approach is to use an additional *lubrication* assumption, namely that the aspect ratio (ratio of the film thickness to characteristic length scale) is also small [6]. This enables the Stokes equations to be rewritten as a fourth-order, non-linear, degenerate, parabolic partial differential equation for the film thickness; evidence accumulated to date [2, 4, 7] suggests that the lubrication approach is sufficiently accurate even in regions of parameter space where it is not strictly valid.

A range of numerical approaches has been used over the past two decades to solve the thin film lubrication equations [8, 9], most based on discrete finite difference/volume analogues solved in a variety of ways; with semi-implicit (ADI) schemes, see [10], proving to be a more popular alternative to explicit ones which are extremely restrictive apropos the choice of time step. At the same time, the need to address problems of a practical nature has spurred the development of an efficient, implicit full approximation storage (FAS) multigrid strategy for solving the discretized lubrication equations for evaporative [11] and non-evaporative [7] flows. Recent results, employing in addition automatic spatial grid adaption [12], have shown the benefits of the latter in restricting the use of fine grids to those regions in and around small, localized topography where very high resolution is required to produce accurate, grid-independent solutions.

This paper demonstrates the benefits of automatic grid refinement in tandem with adaptive time-stepping for the solution of continuous thin film flow problems featuring complex submerged topography and/or small-scale occlusions. The motivation being the key practical need, during micro-electronic component manufacture [2], to minimize free-surface disturbances. The effect of flow orientation is explored for the first time; while the benefits of automatic grid adaptivity in terms of solution accuracy when mesh refinement becomes critical as topographic features are miniaturized, as often encountered in practice, are clearly demonstrated.

2. PROBLEM DESCRIPTION

2.1. Mathematical model

Figure 1 schematically illustrates the motion of a thin liquid film, $H(X, Y, T)$, of asymptotic thickness H_0 over a flat substrate, containing a small circular protrusion ($0 \leqslant S_0 \ll H_0$) or occlusion ($S_0 \gg H_0$), of radius R_T, inclined at an angle θ to the horizontal, with a constant volumetric flow Q_0 per unit width.

The liquid is assumed to be inertialess, Newtonian and incompressible, with constant density, ρ, viscosity, μ and surface tension, σ, and its motion therefore governed by the Stokes and continuity equations, viz

$$\rho \frac{\partial \underline{U}}{\partial T} = -\nabla P + \mu \nabla^2 \underline{U} + \rho \underline{g}, \quad \nabla \cdot \underline{U} = 0 \tag{1}$$

where $\underline{U} = (U, V, W)$ and P are the fluid velocity and pressure, respectively, T is time and $\underline{g} = g(\sin\theta, 0, -\cos\theta)$ is the acceleration due to gravity.

DOI: 10.1002/fld

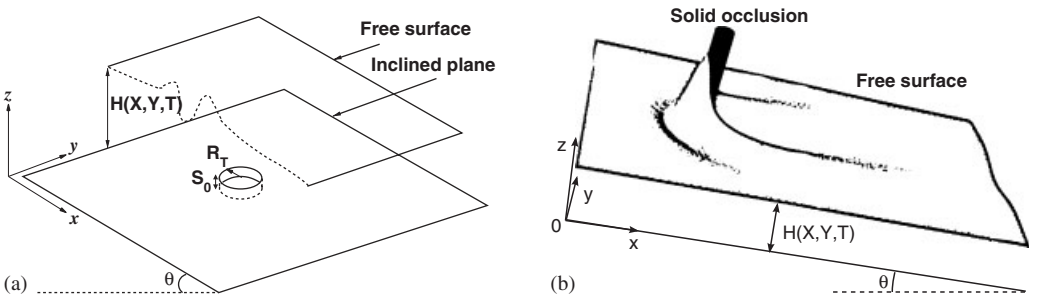

Figure 1. The gravity-driven flow: (a) over a small circular protrusion and (b) past a circular occlusion.

Assuming that $\varepsilon = H_0/L_0$ is small, where L_0 is the characteristic length scale, yields the following equations for non-dimensional film thickness, h, and pressure, p

$$\frac{\partial h}{\partial t} = \frac{\partial}{\partial x}\left[\frac{h^3}{3}\left(\frac{\partial p}{\partial x} - 2\right)\right] + \frac{\partial}{\partial y}\left[\frac{h^3}{3}\left(\frac{\partial p}{\partial y}\right)\right] \tag{2}$$

$$p = -\frac{6}{\beta^3}\nabla^2(h+s) + \frac{2}{\beta}6^{1/3}N(h+s) \tag{3}$$

where $L_0 = \beta(\sigma H_0/3\rho g \sin\theta)^{1/3}$, $\beta = L_0/L_c$, with L_c the capillary length, s is the topography/pattern height and N measures the influence of gravity on the free-surface shape. Further details, including the scalings employed, are given in [7].

2.2. Boundary conditions

Fully developed flow conditions are specified at the inflow and outflow boundaries, while tangential flow conditions are imposed at the span-wise boundaries, $y = 0$ and 1. In addition, the static wetting curve, $h_w(x, y)$, where the fluid meets the surface of a solid occlusion is defined such that

$$\nabla h_w \cdot \underline{n} = \tan\left(\frac{\pi}{2} - \theta_s\right) \tag{4}$$

where $\underline{n}$ is the outward pointing unit normal at the occlusion surface and θ_s is the static contact angle, taken to be $\pi/2$. The no-slip condition on the occlusion is imposed by specifying zero volumetric flux across its surface.

3. NUMERICAL METHOD

The lubrication equations (2) and (3) are solved on a computational domain, with equal, uniform grid spacings, Δ, in the x- and y-directions with adaptive time integration utilizing the standard, second-order accurate Crank–Nicholson method employing temporal error control *via* predictor–corrector stages, see [13].

In the multigrid method, a sequence of progressively finer grids ($\mathcal{G}_k$: $k = 0, 1, \ldots, K$) is defined with uniform grid spacing Δ_k. Each $\mathcal{G}_k$ has $n_k = 2^{k+c+1} + 1$ nodes per unit length in each

DOI: 10.1002/fld

co-ordinate direction where c is a constant defining the resolution of the coarsest grid level, so that $\Delta_k = 2^{-(k+c+1)}$. The results were obtained using a full multigrid V(2, 2) cycle, a coarse grid parameter $c = 2$ and an underlying coarse global grid with $k = 1$ corresponding to a uniform grid spacing $\Delta_1 = \frac{1}{16}$. Automatic adaptive grid refinement was implemented if the relative truncation error $\tau_k^{k-1} \geqslant \varepsilon$, where ε is a user-specified tolerance. The reader may refer to [12] for a more comprehensive description of the formulation and strategy involved.

4. RESULTS

The first problem considered is the flow of water films of asymptotic film thickness, $H_0 = 100\,\mu\text{m}$, viscosity, 0.001 Pa s, density, $\rho = 1000\,\text{kg m}^{-3}$ and surface tension, $\sigma = 0.07\,\text{N m}^{-1}$ down a substrate inclined at 30° to the horizontal and with a constant inlet flow rate, $Q_0 = 1.635 \times 10^{-6}\,\text{m}^2\,\text{s}^{-1}$ [2], over simple and multiple connected circuits. The former is illustrated in Figure 2, for a simple dumb-bell circuit of length 10.9 mm, width 3.6 mm and height 30 μm, constructed by combining and subtracting circular and rectangular primitives—simpler examples of which are discussed in [12]. The results show how the solution adapts around the topography where a *bow wave* disturbance is shed from each circular end. The effect of circuit orientation on the amplitude of the free-surface disturbance is shown in Figure 3, in alignment with the flow direction corresponding to 0° of orientation. The minimum amplitude of the free-surface disturbance (6.5%) occurs at an orientation of approximately 0° (Figure 2(b)), while a maximum disturbance of 8.8% occurs at approximately 75° (Figure 3(a)). Such information is of considerable value to circuit designers and manufacturers, who are constrained by strict tolerance requirements during photo-lithographic processing [2]. The flexibility of the adaptive scheme is further demonstrated in Figure 4 for a more realistic test case.

The second problem investigated explores the benefits of grid adaptivity for the flow of a thin water film, $H_0 = 10\,\mu\text{m}$, past a solid occlusion of elliptical cross-section with semi-major and minor

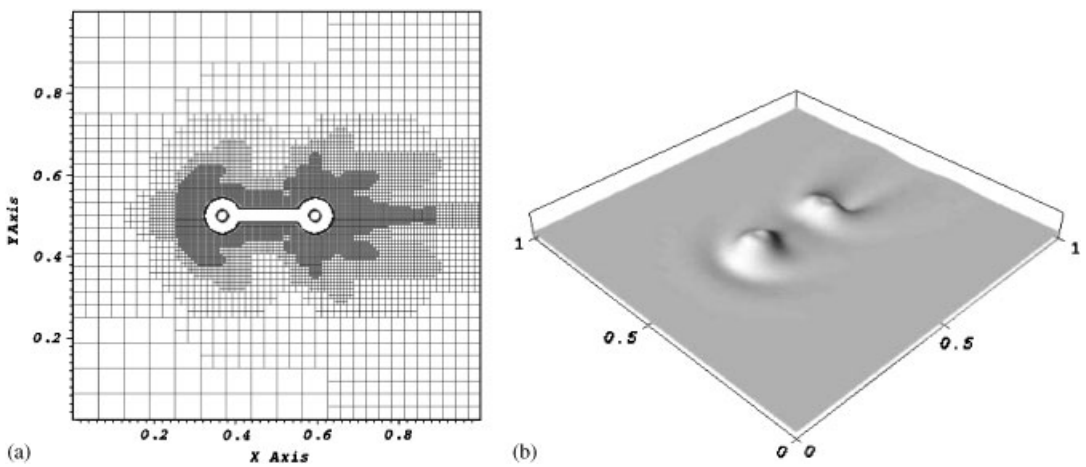

Figure 2. The flow (left to right) over a simply connected dumb-bell circuit topography: (a) final adaptive mesh structure and (b) resulting free-surface shape.

DOI: 10.1002/fld

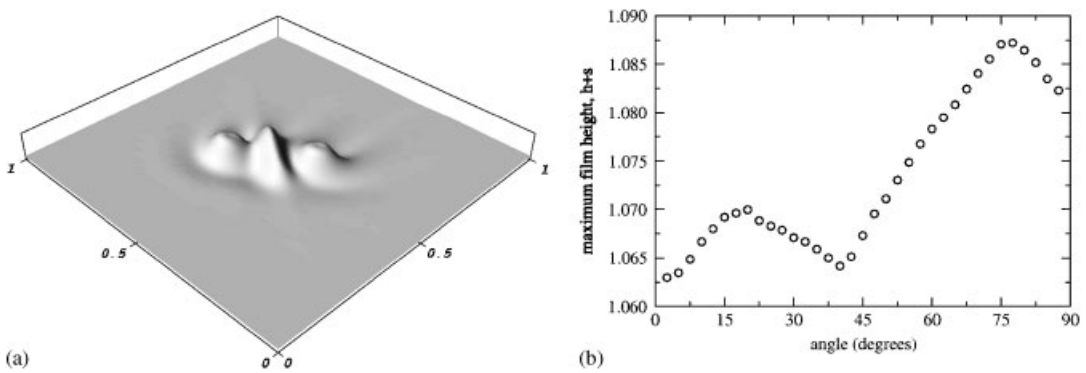

Figure 3. (a) The resultant free-surface shape for flow (left to right) over a simply connected dumb-bell circuit topography orientated at an angle of 75° and (b) the effect of flow orientation with respect to the magnitude of the maximum free-surface disturbance.

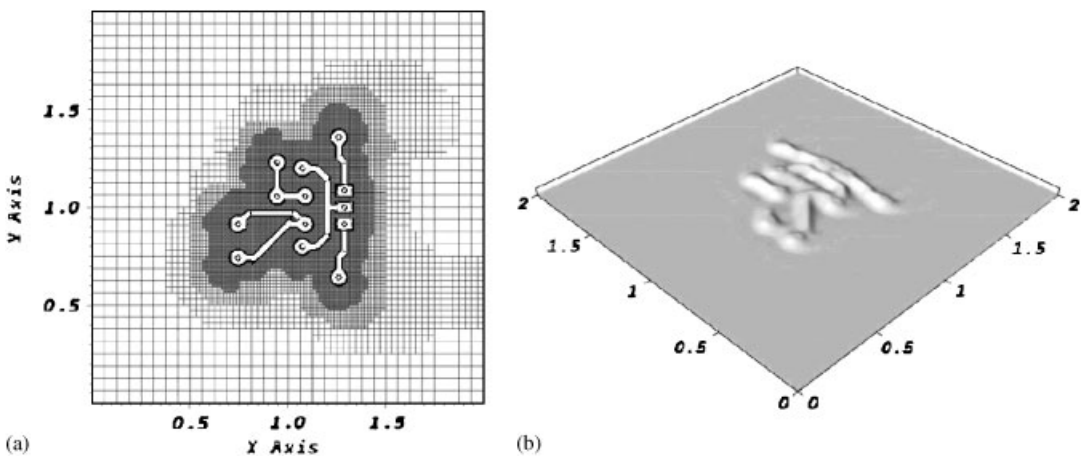

Figure 4. The flow (left to right) over a complex multiply-connected circuit topography: (a) final adaptive mesh structure and (b) resultant free-surface shape.

axes of 145 and 72 μm, respectively. The extent of the solution domain is 14.4 mm × 7.2 mm, with a constant inlet flow rate per unit length, $Q_0 = 1.635 \times 10^{-9}\,\mathrm{m^2\,s^{-1}}$. The inset in Figure 5(b) shows that a finest adaptive grid level of $k = 7$ ($\Delta_7 = \frac{1}{1024}$) is needed to ensure a mesh-independent solution. For this flow problem, the adaptive solver is found to be extremely efficient since it requires only 14 400 nodes, as compared with over 2 million nodes for a corresponding non-adaptive solution having the same accuracy; resulting in a 90% reduction in CPU time. Such savings are vital, particularly when more practical problems with densely packed topographic features need to be addressed.

DOI: 10.1002/fld

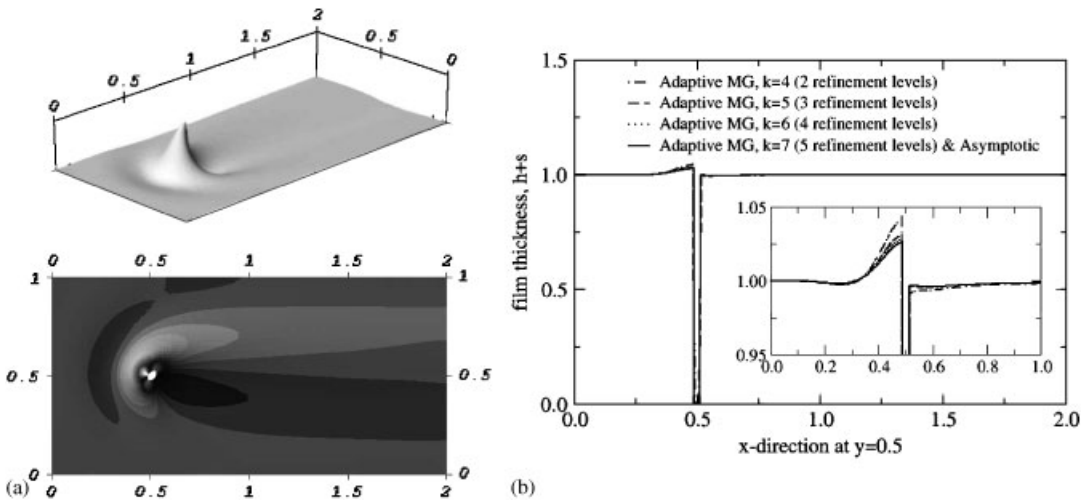

Figure 5. Flow (left to right) past a small skewed (45°) elliptical occlusion located at $(x, y) = (0.5, 0.5)$: (a) resulting free-surface shape and its associated iso-contour profile and (b) stream-wise free-surface profile along $y = 0.5$.

5. DISCUSSION

The flow of continuous thin liquid films over topography has many practical applications in a variety of biological, scientific and industrial processes. However, until now the numerical solution of such problems has been restricted to idealized cases with simple topographic structure whose in-plane length scales are significantly larger than that frequently encountered in practice. An adaptive multigrid strategy, such as the one utilized here, with the flexibility to create complex topographic patterns from basic primitives, can be used to explore the issue of flow orientation in the case of complex and multiply-connected submerged circuit topographies; indeed, even for the case of a simple dumb-bell circuit, poor flow orientation is found to lead to a 35% enhancement in the magnitude of the resulting free-surface disturbance. It is also shown to offer significant efficiency gains over existing ADI and non-adaptive multigrid solvers, in particular when fine mesh resolution is essential for the generation of accurate grid-independent solutions when a small-scale topography/occlusion is encountered. Both of these attributes represent a distinct step forward in the quest to solve thin film flows on real surfaces.

REFERENCES

1. Lee HJ, Michielsen S. Preparation of a superhydrophobic rough surface. *Journal of Polymer Science, Part B: Polymer Physics* 2007; **45**(3):253–261.
2. Decré M, Baret J-C. Gravity-driven flows of viscous liquids over two-dimensional topographies. *Journal of Fluid Mechanics* 2003; **487**:147–166.
3. Demirci U. Picoliter droplets for spinless photoresist deposition. *Review of Scientific Instruments* 2005; **76**:065103.
4. Mazouchi A, Homsy GM. Free surface Stokes flow over topography. *Physics of Fluids* 2001; **13**:2751–2761.
5. Blyth MG, Pozrikidis C. Film flow down an inclined plane over a three-dimensional obstacle. *Physics of Fluids* 2006; **18**:052104.

DOI: 10.1002/fld

6. Oron A, Davis S, Bankoff S. *Reviews of Modern Physics* 1997; **69**:931.
7. Gaskell PH, Jimack PK, Sellier M, Thompson HM, Wilson MCT. Gravity-driven flow of continuous thin liquid films on non-porous substrates with topography. *Journal of Fluid Mechanics* 2004; **509**:253–280.
8. Kondic L, Diez J. Instabilities in the flow of thin films on heterogeneous surfaces. *Physics of Fluids* 2004; **16**(9):3341–3360.
9. Becker J, Grun G, Seemann R, Mantz H, Jacobs K, Mecke KR, Blossey R. Complex dewetting scenarios captured by thin-film models. *Nature Materials* 2003; **2**:59–63.
10. Schwartz LW, Roux D, Cooper-White JJ. On the shapes of droplets that are sliding on a vertical wall. *Physica D*: *Nonlinear Phenomena* 2005; **209**(1–4):236–244.
11. Gaskell PH, Jimack PK, Sellier M, Thompson HM. Flow of evaporating, gravity-driven thin liquid films over topography. *Physics of Fluids* 2006; **18**(1):013601.
12. Lee YC, Thompson HM, Gaskell PH. An efficient adaptive multigrid algorithm for predicting thin film flow on surfaces containing localized topographic features. *Computers are Fluids* 2007; **36**:838–855.
13. Gaskell PH, Jimack PK, Sellier M, Thompson HM. Efficient, accurate time adaptive multigrid simulations of droplet spreading. *International Journal for Numerical Methods in Fluids* 2004; **45**:1161–1186.

DOI: 10.1002/fld